HARMONIC ANALYSIS OF PRECIPITATION DATA IN EASTERN IDAHO

Thomas A. Andretta

NOAA/National Weather Service Office
Pocatello/Idaho Falls, Idaho

Abstract

Seasonal cycles of precipitation are documented for eastern Idaho using observed National Weather Service (NWS) climate station data available from the NOAA / National Climatic Data Center (NCDC) in Asheville, North Carolina. In order to better detect the seasonal precipitation patterns in the mountains of eastern Idaho, this study further utilized data obtained from 33 automated SNOTEL sites archived at the National Resources Conservation Service (NRCS). Harmonic analysis is applied to both data sets, identifying seasonal variabilities in their precipitation time series and associated climate regimes in eastern Idaho. The arithmetic means, standard deviations, percentage contributions of six harmonic amplitudes and harmonic phase values are computed for the station network. Cold season first harmonic maxima related to Pacific cyclonic controls are located in the Magic Valley, west Central Mountains, and Upper Snake Highlands while warm season maxima influenced by convection occur over the remainder of the Central Highlands. A transition in climate regimes is apparent in the Lower Snake River Plain (LSRP) with dominant first harmonic amplitudes replaced by strong second harmonic values in the Upper Snake River Plain (USRP). A large area of prominent third harmonic amplitudes, possibly linked to large-scale topographic forcing, is observed from the eastern part of the USRP to the Idaho-Wyoming border and extending south into the Caribou Highlands. Southeast of the Central Mountains, well-defined fourth harmonic amplitudes are located near the intersection of the Big and Little Lost River Valleys and the USRP where local upslope and convergence are factors in producing precipitation. Harmonic analysis will assist operational forecasters in identifying the phase, strength, and location of seasonal precipitation regimes over eastern Idaho.

1. Introduction

This study employs mean monthly precipitation time series across the intermountain West for eastern Idaho and the contiguous areas of Montana, Utah, and Wyoming to elucidate seasonal changes in rainfall and snowfall patterns. Mean monthly precipitation normals are derived from 30 year (1961 to 1990) National Weather Service (NWS) data and 10 to 15 year National Resources Conservation Service (NRCS) SNOTEL data. Tables 1a, 1b, and 1c provide a complete listing of the NWS and NRCS climate stations included in this analysis, indexed by acronym, name, longitude, latitude, and elevation.

Harmonic analysis is applied to the NWS and NRCS mean monthly precipitation time series data of each station. This technique has several advantages over using common statistics. The annual march or time series for each station can be deduced into an arithmetic mean plus several harmonic time series. The harmonics allow a quantifiable way of delineating the different variabilities or tendencies in the data. These tendencies may be categorized as annual (one maximum and one minimum), semi-annual (two maxima and two minima) and so on. The tendencies are classified by two parameters: harmonic amplitude and phase. The harmonic amplitude indicates the strength of the particular tendency while the phase indicates the time the harmonic reaches a maximum or minimum. Transitions in phase corresponding to large harmonic amplitudes represent seasonal changes in precipitation regimes. However, harmonics do not handle step functions adequately and abrupt changes between seasons can sometimes occur in the phase charts. Nevertheless, the amplitude and phase trends in the time series data can easily be detected both numerically and graphically by using harmonic analysis.

2. Eastern Idaho Terrain Features

Figure 1 displays the topography map of eastern Idaho with geographical regions indexed by number. NWS and NRCS station identifiers, located by the dashed meridians and parallels, are illustrated on a map of eastern Idaho in Fig. 2. The terrain of eastern Idaho is largely influenced by the Snake River Plain (SRP) which is approximately 100 km wide, oriented from southwest to northeast with a gradual increase in elevation from ~1.3 km near Minidoka (MIN) (in the Magic Valley) to ~1.5 km near St. Anthony 1 WNW (STA). The region of the SRP north of Blackfoot 2 SSW (BLK) to Arco 3 SW (ARC) is defined as the Upper Snake River Plain (USRP), and the region south to American Falls 1 SW (AMF) and MIN is defined as the Lower Snake River Plain (LSRP). Other important geographical features include: the Upper Snake and Caribou Highlands (average elevation ~2.0 km), which define the northeast and southeast boundary of the USRP and LSRP, respectively; the Central Mountains (average elevation ~3.0 km) which define the west and northwest boundary of the USRP and LSRP; and the relatively deep and narrow Central Mountain Valleys (Big Lost River, Little Lost River, and Birch Creek) which are oriented from northwest to southeast and open onto the USRP. These Central Mountain Valleys

Table 1a. NWS Climate Stations in Eastern Idaho

Abbreviation	Station Name	Longitude (W)	Latitude (N)	Elevation (m)
ABD	Aberdeen Experimental Station	112.83	42.95	1342
AMF	American Falls 1 SW	112.87	42.78	1316
ARB	Arbon 2 NW	112.50	42.50	1576
ARC	Arco 3 SW	113.33	43.60	1624
ASH	Ashton	111.45	44.06	1603
BLK	Blackfoot 2 SSW	112.35	43.17	1368
BLS	Bliss 4 NW	115.00	42.95	998
BYI	Burley FAA Airport	113.77	42.53	1267
CHA	Challis	114.23	44.50	1577
CHL	Chilly Barton Flat	113.82	43.98	1908
COB	Cobalt	114.23	45.08	1527
CRA	Craters of the Moon Park	113.57	43.47	1797
DRG	Driggs	111.12	43.73	1879
DUB	Dubois Experimental Station	112.20	44.25	1661
FFD	Fairfield Ranger Station	114.78	43.35	1544
FOH	Fort Hall Indian Agency	112.43	43.03	1359
GRA	Grace	111.73	42.58	1692
GRS	Grouse	113.62	43.70	1859
SUN	Hailey 3 NNW	114.33	43.57	1653
HAM	Hamer 4 NW	112.27	43.97	1438
HZN	Hazelton	114.13	42.60	1238
HIL	Hill City 1 W	115.05	43.30	1524
HLS	Hollister	114.57	42.35	1379
HOW	Howe	113.00	43.78	1469
ID1	Idaho Falls 2 ESE	112.02	43.48	1452
ID2	Idaho Falls 16 SE	111.78	43.35	1783
ID3	Idaho Falls FAA Airport	112.07	43.52	1442
ID4	Idaho Falls 46 W	112.95	43.37	1505
ISL	Island Park	111.37	44.42	1917
JRM	Jerome	114.52	42.73	1140
LIF	Lifton Pumping Station	111.30	42.12	1806
MAC	Mackay Ranger Station	113.62	43.92	1797
MLD	Malad City	112.28	42.17	1362
MAL	Malta 2 E	113.28	42.30	1384
MAY	May	113.92	44.60	1558
MIN	Minidoka Darn	113.48	42.67	1280
MTP	Montpelier Ranger Station	111.30	42.32	1817
OAK	Oakley	113.88	42.23	1402
PAL	Palisades	111.23	43.37	1641
PAU	Paul 1 ENE	113.75	42.62	1283
PIC	Picabo	114.07	43.30	1486
PIH	Pocatello WSO Airport	112.60	42.92	1358
RIC	Richfield	114.15	43.06	1312
SMN	Salmon KSRA	113.90	45.18	1198
SHO	Shoshone 1 WNW	114.43	42.97	1204
STA	Saint Anthony 1 WNW	111.72	43.97	1509
STN	Stanley	114.93	44.22	1911
SWV	Swan Valley 2 E	111.30	43.45	1634
TET	Tetonia Experimental Station	111.27	43.85	1881
TWF	Twin Falls WSO	114.35	42.55	1207

decrease in elevation from ~1.9 km at their northwest end to ~1.6 km at the opening to the USRP. Data collection sites are generally collocated with populated valley locations, but terrain heights go well above 2.0 km in most mountainous areas in eastern Idaho (Fig. 1).

Table 1b. NWS Climate Stations in Montana, Utah, and Wyoming

Abbreviation	Station Name	Longitude (W)	Latitude (N)	Elevation (m)
DLN	Dillon Airport, MT	112.55	45.25	1590
LAK	Lakeview, MT	111.80	44.60	2045
LIM	Lima, MT	112.58	44.65	1912
MOD	Monida, MT	112.32	44.57	2068
WEY	West Yellowstone, MT	111.10	44.65	2030
GAR	Garland, UT	112.17	41.73	1326
GRC	Grouse Creek, UT	113.88	41.72	1622
LKN	Laketown, UT	111.32	41.82	1822
LOG	Logan, UT	111.80	41.75	1460
PRK	Park Valley, UT	113.33	41.82	1689
RCH	Richmond, UT	111.82	41.90	1426
SNW	Snowville, UT	112.72	41.97	1390
AFT	Afton, WY	110.93	42.73	1893
ALT	Alta 1 NNW, WY	111.03	43.78	1960
JAC	Jackson, WY	110.77	43.48	1899
MOS	Moose, WY	110.72	43.67	1972
YPK	Yellowstone Park, WY	110.70	44.97	1899

3. Methodology

Horn and Bryson (1960) used harmonic analysis to study the seasonal cycles in precipitation over the conterminous United States using station data from the period 1921 to 1950. Fitzpatrick (1964) and Hastenrath (1968) used the method to examine rainfall trends over Australia and Central America, respectively. Moreover, Scott and Shulman (1979) and Winkler et al. (1988) applied harmonic analysis to observed precipitation in the United States. On a much smaller geographical scale, this technique was used to examine diurnal precipitation signatures in the Salt Lake Valley (Astling 1984). Kirkyla and Hameed (1989) investigated seasonal cycles of precipitation using gridded precipitation data both from observations and the 1 x CO_2 run of the Oregon State University Global General Circulation Model (OSU GCM) for the 48 conterminous United States and other geographical areas (Potter and Gates 1984). A follow-up study by Andretta (1990) utilized harmonic analysis to analyze the CO_2-induced precipitation perturbations in North America and Africa using the OSU GCM.

This technique uses sine and cosine trigonometric functions to explain the finite time series periodic nature of temporally varying parameters (Panofsky and Brier 1958; Wilks 1995). Summing over the k={1,2,3,...,N/2} harmonics, the net equation for the time series becomes:

$$Y(t) = Y_o + \Sigma A_k \cos(360N(t-t_k)/2P) \qquad (1)$$

where, Y(t) is the sum of Y_o, the arithmetic mean monthly value of the N observations, plus a time series of k harmonics; P is the total period covered by the harmonics. Each of the k harmonics (with frequency k) has an A_k net harmonic amplitude and a time, t, when this amplitude reaches it's maximum value ($t=t_k$). The

Table 1c. NRCS SNOTEL Stations in Eastern Idaho

Abbreviation	Station Name	Longitude (W)	Latitude (N)	Elevation (m)
BEC	Bear Canyon	113.93	43.75	2409
BRS	Bosteter Ranger Station	114.18	42.17	2287
CRC	Crab Creek	112.00	44.43	2091
DLS	Dollar Hide Summit	114.67	43.60	2567
EMS	Emigrant Summit	111.57	42.37	2253
FBS	Franklin Basin	111.60	42.05	2491
GNA	Galena	114.67	43.88	2268
GLS	Galena Summit	114.72	43.85	2677
GAR	Garfield Ranger Station	113.93	43.62	2000
GIV	Giveout	111.17	42.42	2113
HCK	Hilts Creek	113.47	44.02	2439
HOC	Howel Canyon	113.62	42.32	2433
HUM	Humboldt Gulch	115.78	47.53	1296
HYN	Hyndman	114.17	43.70	2268
IPR	Island Park Ranger Station	111.38	44.42	1918
LOK	Lookout	115.70	47.45	1567
LOL	Lost Lake	115.97	47.08	1863
LWD	Lost Wood Divide	114.27	43.83	2409
MGM	Magic Mountain	114.30	42.18	2098
MEL	Meadow Lake	113.32	44.43	2790
MCS	Mill Creek Summit	114.47	44.47	2683
MSE	Moonshine	113.42	44.42	2268
MOC	Moose Creek	113.95	45.67	1890
MGC	Morgan Creek	114.27	44.85	2317
OXF	Oxford Spring	112.13	42.27	2055
SHM	Sheep Mountain	111.68	43.22	2003
SGC	Slug Creek Divide	111.30	42.57	2203
SOR	Somsen Ranch	111.37	42.95	2073
STM	Stickney Mill	114.22	43.87	2265
SWP	Swede Peak	113.97	43.62	2329
VIM	Vienna Mine	114.85	43.80	2732
WHE	White Elephant	111.42	44.53	2351
WLD	Wildhorse Divide	112.48	42.75	1979

harmonic phase value, t_k, of the net kth harmonic amplitude, A_k, is written as:

$$t_k = (P/360k)(180/\Pi)\arctan(B_k/C_k) + (P/k) \qquad (2)$$

In (2), $\Pi = 3.1415927$ and the net harmonic amplitudes, A_k, can be written as a function: $A_k = (B_k^2 + C_k^2)^{1/2}$. A scaling factor, P/k, is used to ascertain the correct harmonic phase solution. By summing over all of the t={1,2,3,...,N} observations and the k={1,2,3,...,N/2} harmonics, the least-squares approximations of the harmonic amplitudes, B_k and C_k, are computed as:

$$B_k = 2/N\ \Sigma\Sigma[y_t \sin(360kN/P)] \qquad (3)$$

and

$$C_k = 2/N\ \Sigma\Sigma[y_t \cos(360kN/P)] \qquad (4)$$

For this study, N=12 observations corresponding to the 12 mean monthly data values. The monthly normals are divided into equal periods of 30.44 days. The period of the observations is 1 year or P=12 months. Each of the y_t correspond to the t={1,2,3,...,12} mean monthly precipitation amounts, in units of inches per month. The net harmonic amplitude, A_k, is converted to a percent with the magnitudes corresponding to the harmonic strengths. There are a total of k=N/2=6 harmonic amplitudes and phase values. The kth harmonic curve features a kth maximum (or frequency) every N/k=12/k months.

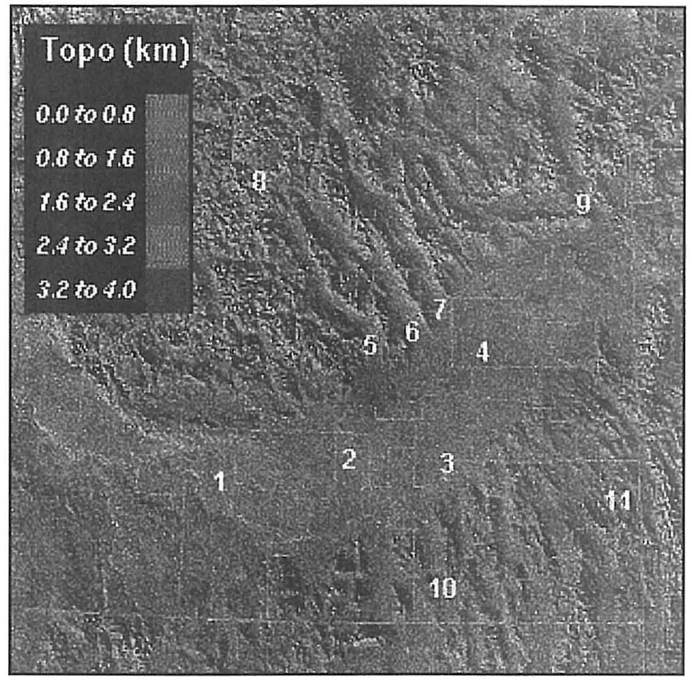

Fig. 1. Topography of Eastern Idaho. (Code: 1 = Western Magic Valley; 2 = Eastern Magic Valley; 3 = Lower Snake River Plain; 4 = Upper Snake River Plain; 5 = Big Lost River Valley; 6 = Little Lost River Valley; 7 = Birch Creek Valley; 8 = Central Mountains; 9 = Upper Snake Highlands; 10 = South Central Highlands; 11 = Caribou Highlands)

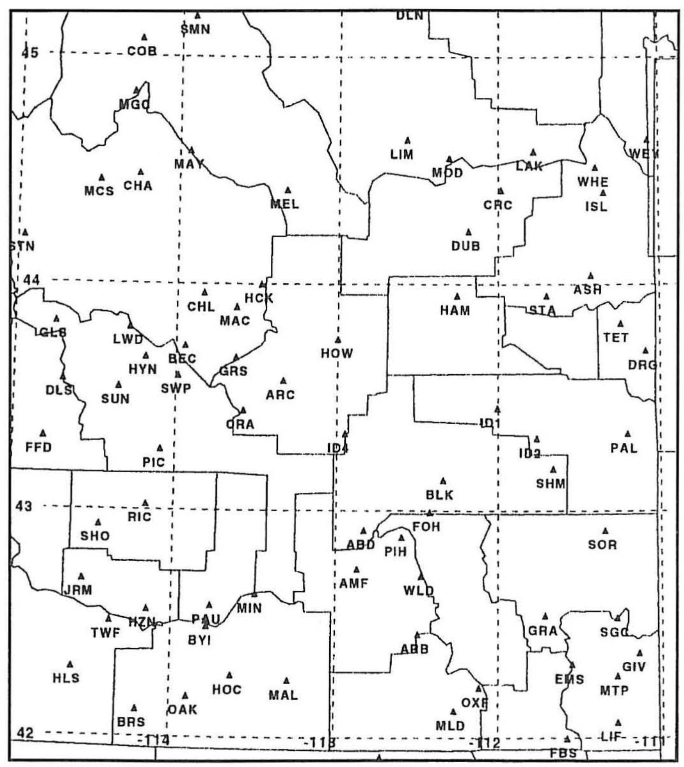

Fig. 2. NWS and NRCS station identifier map of Eastern Idaho

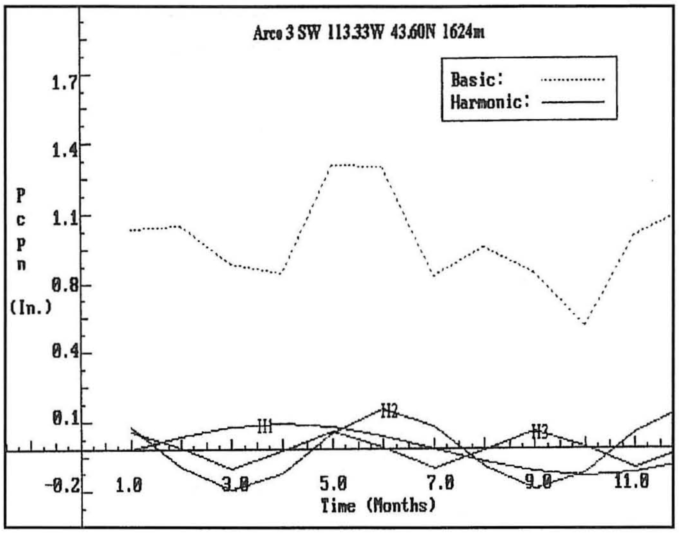

Fig. 3. Precipitation (in.) and harmonic time series for Arco 3 SW

An example of a time series curve for Arco 3 SW, depicting the first three harmonics, which account for 70% of the variability in the time series, is shown in Fig. 3. The dotted curve (labeled "Basic") denotes the mean monthly precipitation time series (inches per month) while the solid curves represent associated harmonics (labeled "Harmonic") indicated by the respective harmonic number, Hk. The first harmonic (H1) clearly shows a tendency for a wet first-half with a drier second-half of the year. The late spring and winter maxima are reflected in the second harmonic curve (H2). Precipitation maxima in January, May, and September are resolved by the third harmonic time series curve (H3).

4. Precipitation Data Analysis

a. The mean monthly precipitation and standard deviation charts

The mean monthly precipitation amounts (Fig. 4) are primarily governed by two variables: elevation and exposure. Elevated locations typically record higher precipitation amounts versus valleys; the complementary effect of elevation and exposure (e.g., orographic upslope) only adds further to the precipitation amounts in the mountains. Figure 4 shows the relatively low precipitation amounts (below 1.0 inch per month) in the USRP and LSRP. While prevailing synoptic mid-level westerly flow occurs over eastern Idaho, the downsloping surface northeast flow around the summertime Great Basin High induces subsidence, attributing in part to the low valley amounts (Trewartha 1981). Late fall and wintertime Pacific cyclogenesis over the northwest United States is a key factor in generating relatively higher precipitation amounts over the mountainous regions of eastern Idaho. For example, in the Upper Snake Highlands, 1.0 to 2.5 inches per month of precipitation occur from orographic enhancement during the wet winter months (Kendrew 1922). Similarly, in the South Central

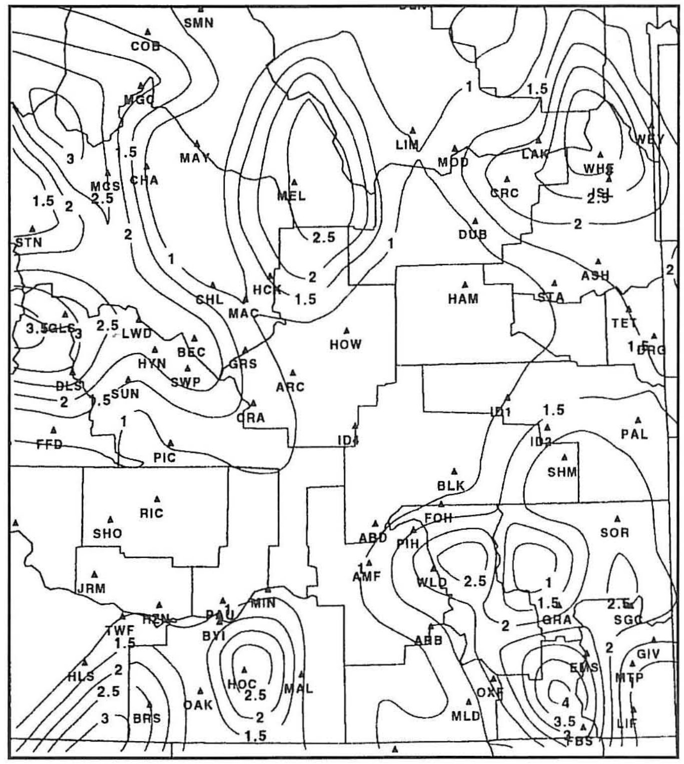

Fig. 4. Mean monthly precipitation (inches)

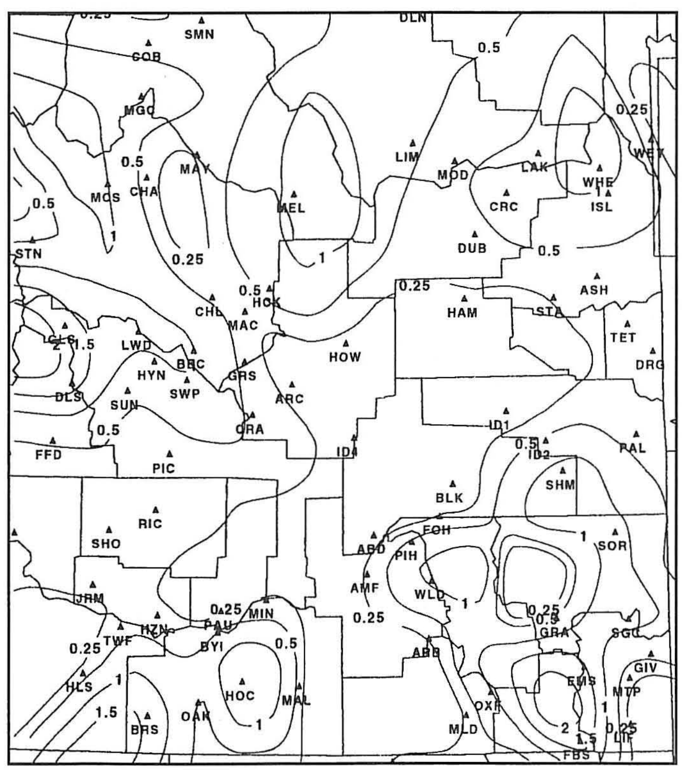

Fig. 5. Standard deviation of the mean monthly precipitation (inches)

Highlands and Caribou Highlands, precipitation amounts average 1.0 to 3.0 inches per month, (locally 4.0 inches per month) as moist west to northwest flow is forced up the east to southeast facing terrain inducing upslope precipitation (Trewartha 1981). Figure 5

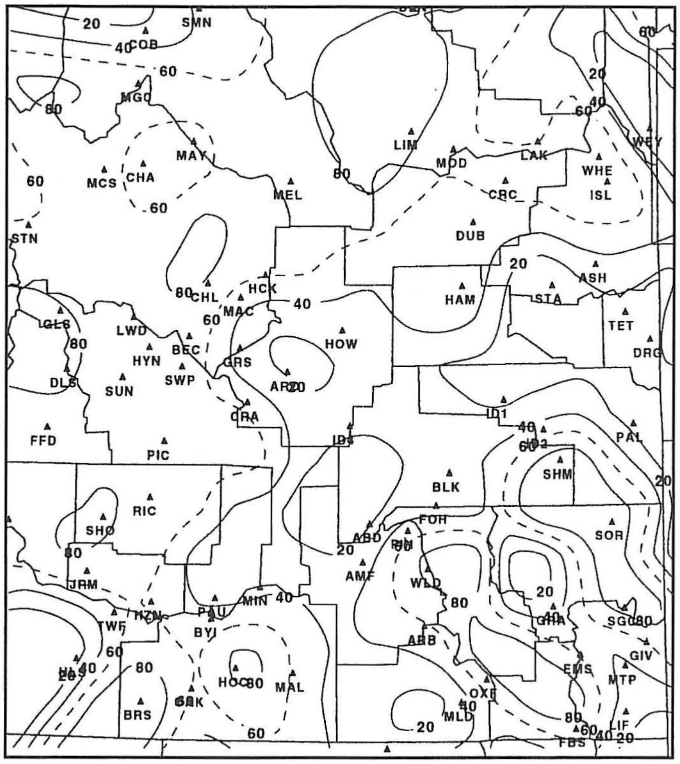

Fig. 6. First harmonic amplitude (percent)

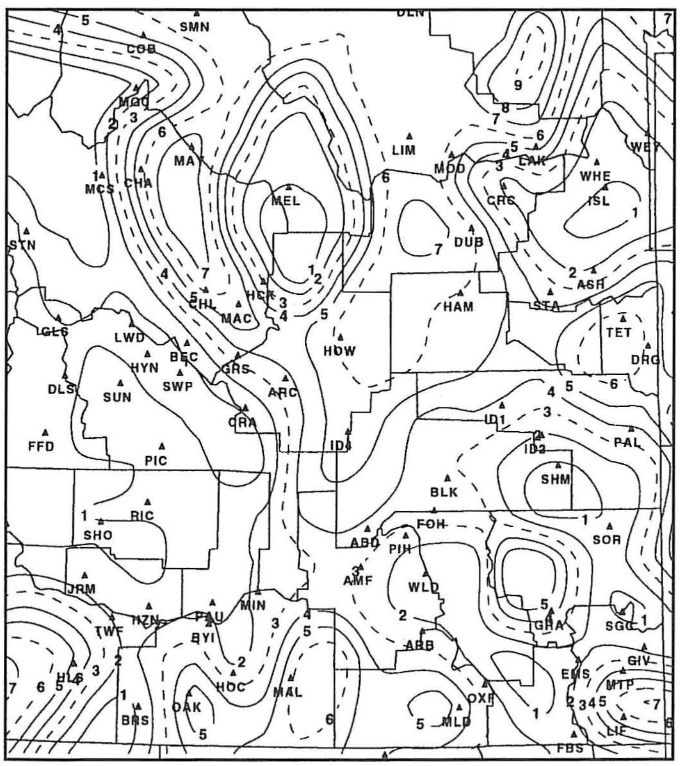

Fig. 7. First harmonic phase (months)

displays the standard deviation for the mean monthly precipitation normals. The higher deviations are generally situated in regions of elevated topography (Fig. 1) where there is greater variability in the seasonal precipitation patterns.

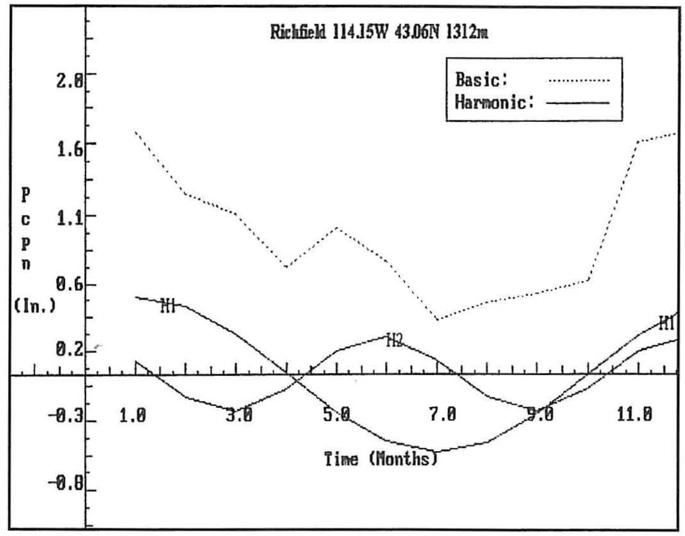

Fig. 8. Precipitation (in.) and harmonic time series for Richfield

b. The first harmonic amplitude percentage and phase charts

The first harmonic amplitude (as a percent) and phase (month of the first harmonic in calendar months) charts represented in Figs. 6 and 7, illustrate the tendency for one maximum and one minimum in the time series data. Dashed contours highlight the beginning months of the four seasons in Fig. 7. Relative to the other harmonics, large first harmonic percentages suggest a strong annual tendency for precipitation in the time series. A large area of strong (60 (dashed line) to 80%) winter maxima covers the Eastern Magic Valley (e.g., Richfield). High first harmonic percentages are also evident in the highlands: Central Mountains (e.g., Stanley (STN)), South Central Highlands (e.g., Howel Canyon (HOC)), near Wildhorse Divide (WLD), east of Oxford Spring (OXF), and in the Upper Snake Highlands near White Elephant (WHE)). In addition, contributions from the first harmonic are large (40 to 60%) over the southern part of the LSRP with maxima during February and March (Fig. 7). The cold season maxima are correlated with winter cyclogenesis associated with the vigorous Aleutian Low and the southward descent of the North Pacific Polar Jet into the Great Basin. (Trewartha 1981). When the eastern Pacific High shifts northward and eastward from early July through August, the SRP experiences increasing subsidence and anticyclonic controls accounting for the dry, late summer period (Trewartha 1981). The time series for Richfield and White Elephant (Figs. 8 and 9, respectively) indicate precipitation maxima from November through January. In these plots, the dotted curve (labeled "Basic") denotes the mean monthly precipitation time series (inches per month) while the solid curves represent associated harmonics (labeled "Harmonic") indicated by the respective harmonic number, Hk. A phase transition from winter to spring to summer maxima occurs across the Central Mountains from Stanley (STN) to Challis (CHA) (Figs. 10 and 11). While both stations show ~55% percent contributions from the first harmonic, a June (t=6) maximum occurs at Challis, while a December (t=12) maximum is noted at

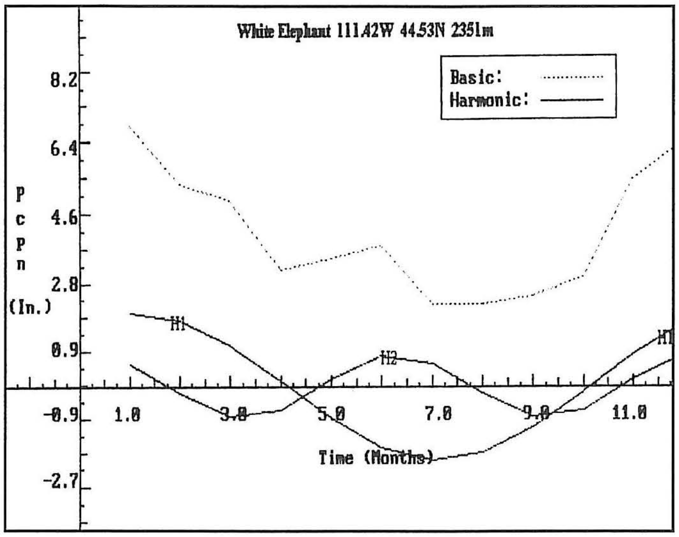

Fig. 9. Precipitation (in.) and harmonic time series for White Elephant

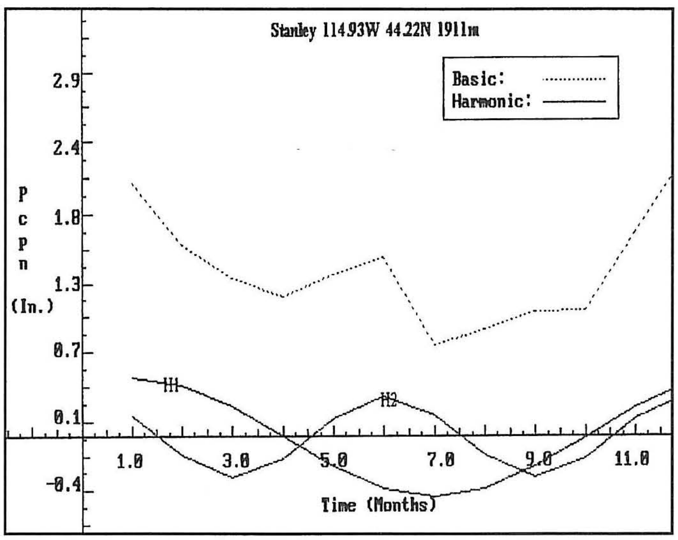

Fig 10. Precipitation (in.) and harmonic time series for Stanley

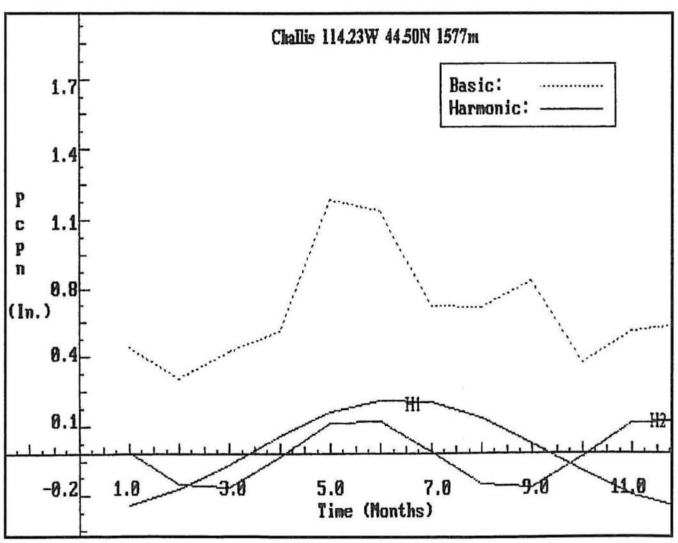

Fig. 11. Precipitation (in.) and harmonic time series for Challis

Stanley. Winter cyclonic controls are more prevalent in the west Central Mountains where elevation and exposure to Pacific moisture help produce precipitation. Conversely, in the east Central Mountains, the influence from summer convection becomes more pronounced versus winter controls because the west Central Mountains remove much of the moisture from the wintertime synoptic-scale flow. A second transition region in first harmonic phase maxima is also noted from a July (t=7) maximum at May (MAY) to a January (t=1) maximum near Meadow Lake (MEL) as winter cyclonic precipitation becomes more important in the annual cycle versus summer convection. The meridionally oriented first harmonic summer maxima which intrudes from southeast of Howe (HOW) to near Lima (LIM) may signal the northward extent of the summer monsoon, which originates over Arizona and New Mexico during June and July (Trewartha 1981). Contributors to late winter February (t=2) and March (t=3) maxima across the LSRP and USRP include snowfall produced by Pacific low pressure systems and in part by post-cold frontal mesoscale winter convergence zones (Andretta and Hazen 1998). The convergence mechanism is orographically-driven and forms when moist air flowing northwesterly through the Big Lost, Little Lost, and Birch Creek Valleys (Fig. 2) merges with southwesterly flow in the SRP, generating clouds and often bands of light to moderate precipitation from between American Falls 1 SW and Blackfoot 2 SSW to near Pocatello WSO Airport (PIH). The strong first harmonics located from American Falls to Arbon 2 NW (ARB) are influenced by this boundary.

c. The second harmonic amplitude percentage and phase charts

The second harmonic amplitude and phase charts are illustrated in Figs. 12 and 13, respectively. These charts indicate the tendency for two maxima and two minima in the annual march of precipitation. Thus, there is a second maximum in Fig. 13 (not shown) which occurs 6 months from the displayed calendar month maximum on this chart. Noteworthy features include an absolute maximum of ~70% located near St. Anthony 1 WNW in the second harmonic amplitude percentage map. A dashed 40% isoline contours the shape of the USRP and LSRP indicating a significant (40 to 70%) contribution from the second harmonic amplitudes in the precipitation time series. Figure 12 also shows a large area of over 50% contributions centered near West Yellowstone, Montana (WEY). The phase chart shows May (t=5) and November (t=11) maxima over most of eastern Idaho (e.g., "Snake River" regime; Kendrew 1922). The strong spring and summer maxima are driven by the northward movement of the North Pacific Polar Jet from the Great Basin into western Canada while the late fall and early winter maxima (November and December) are linked to the southward migration of the jet from western Canada into the Great Basin (Trewartha 1981). The movement of the jet into eastern Idaho causes stronger southwest flow allowing greater exposure to terrain-induced precipitation forcing and a more favorable track for frequent rain/snow-producing Pacific cyclones. Evidence of this trend is provided in the time series of two valley stations, Pocatello WSO Airport and Idaho Falls 2

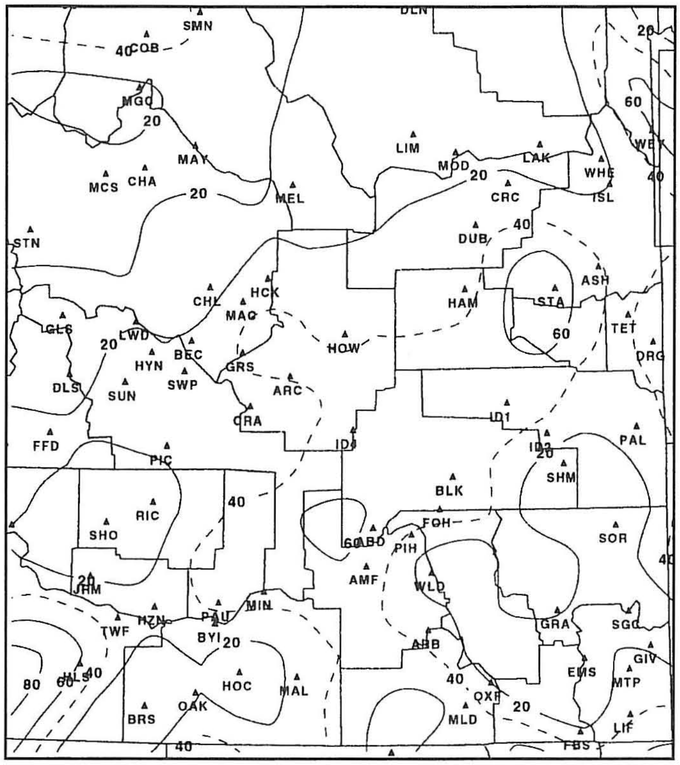

Fig. 12. Second harmonic amplitude (percent)

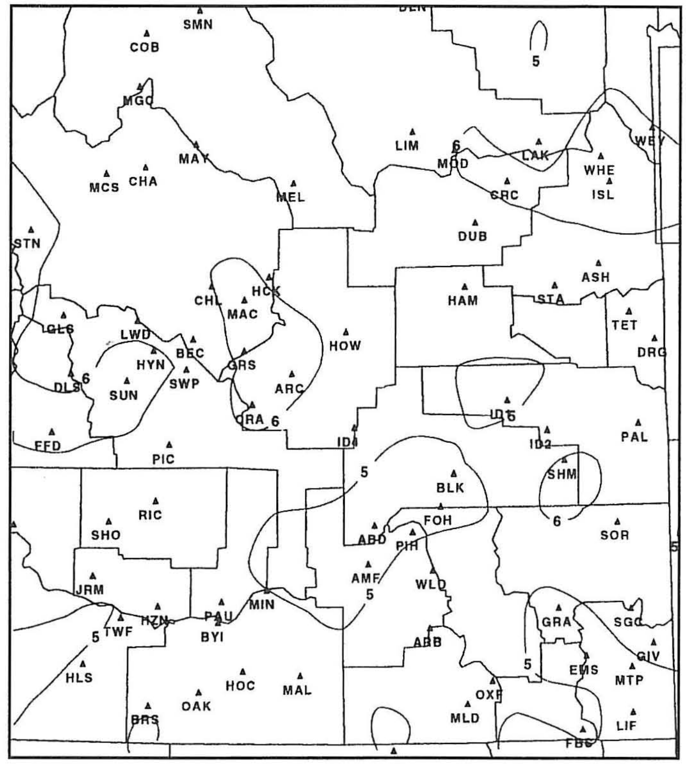

Fig. 13. Second harmonic phase (months)

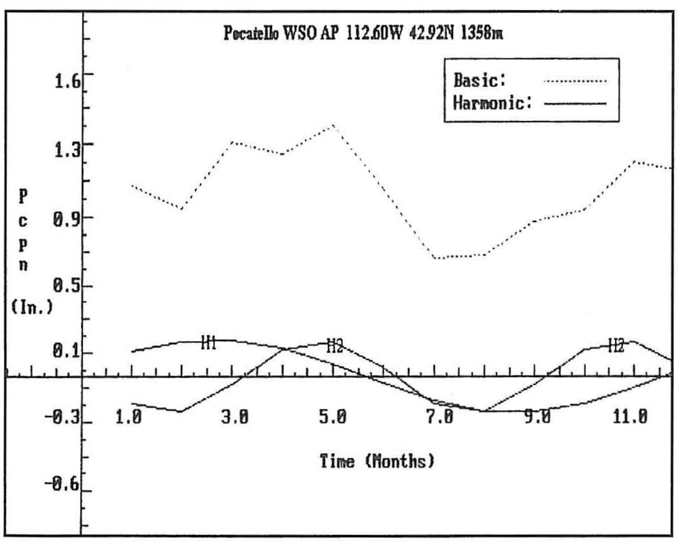

Fig. 14. Precipitation (in.) and harmonic time series for Pocatello WSO AP

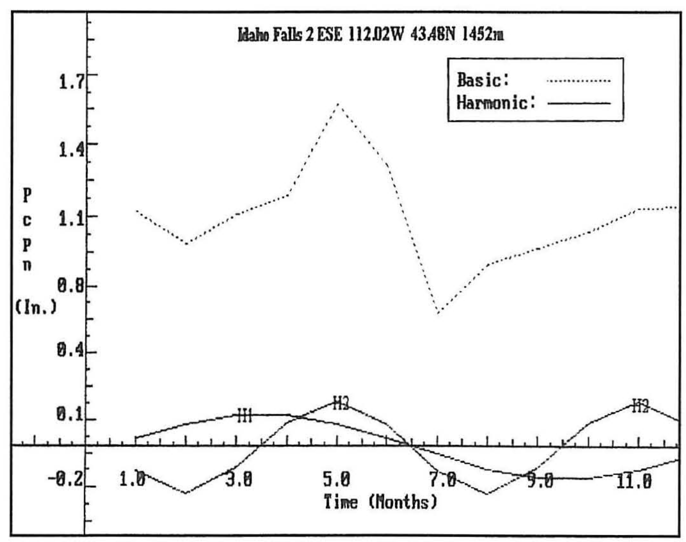

Fig. 15. Precipitation (in.) and harmonic time series for Idaho Falls 2 ESE

ESE (ID1) (Figs. 14 and 15). A semi-annual tendency in the time series data is clearly evident with May (t=5) and November (t=11) maxima. The second harmonic amplitudes also increase in importance as the USRP rises, suggesting a transition in precipitation regimes from strong first harmonic amplitudes over the LSRP (Fig. 5) to a semi-annual precipitation type in the USRP. The May maximum of 1.6 inches peaks at St. Anthony 1 WNW (Fig. 16). In the South Central Highlands (Fig. 1), the time series curve for Malad City (MLD) in Fig. 17 depicts marked May (t=5) and November (t=11) maxima in rainfall. The second harmonic time series for Malad City (H2) constitutes 52% of the annual variability.

d. The third harmonic amplitude percentage and phase charts

The third harmonic amplitude percentage map, Fig. 18, illustrates the importance of three maxima and three minima in the annual march of precipitation. The associated phase map is illustrated in Fig. 19, displaying the calendar month of the third harmonic maximum. (The other two maxima (not shown) occur 4 months before and after this value.) Third harmonic amplitudes are generally small (<20%) across most of eastern Idaho. However, a small area of 20 to 30% contributions covers most of the Caribou Highlands in Fig. 18. A second region of 30 to

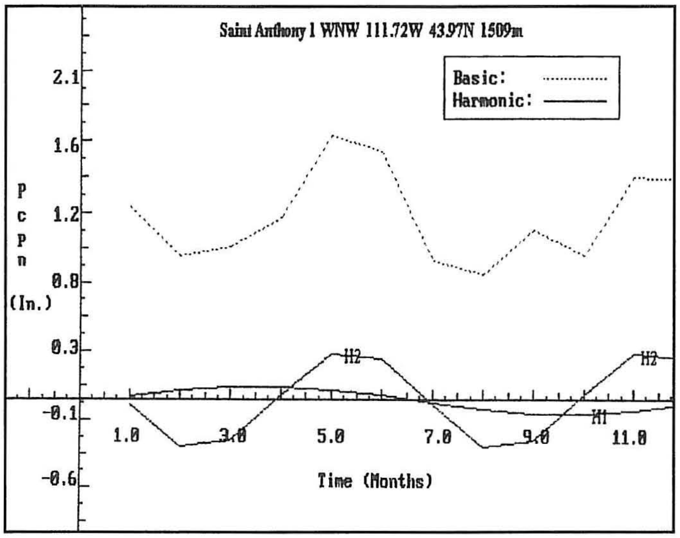

Fig. 16. Precipitation (in.) and harmonic time series for St. Anthony 1 WNW

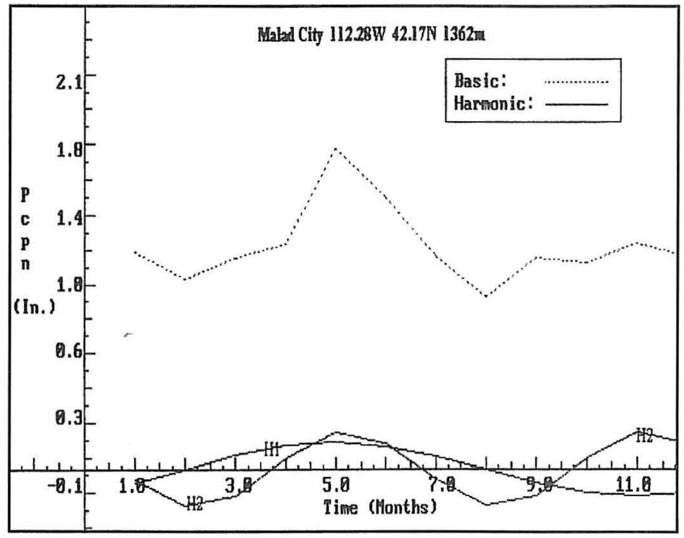

Fig. 17. Precipitation (in.) and harmonic time series for Malad City

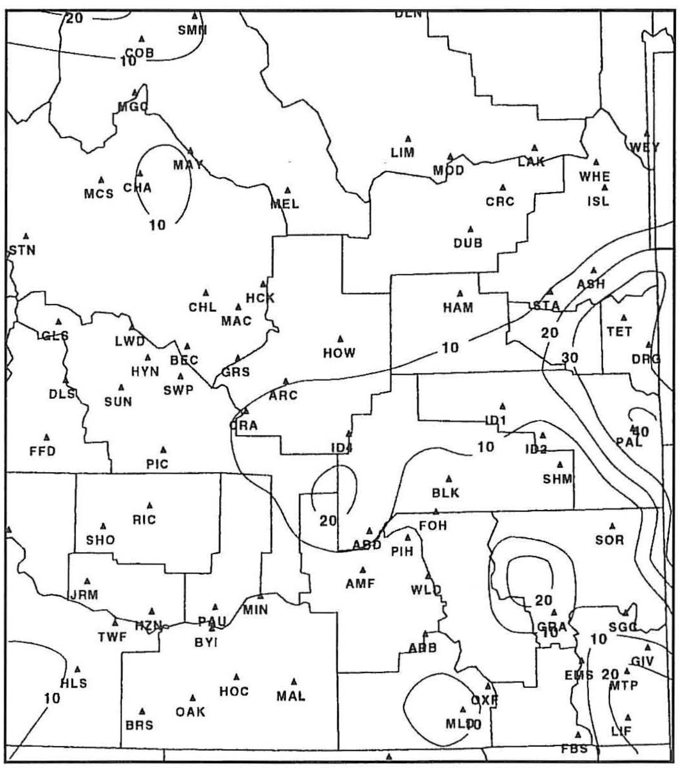

Fig. 18. Third harmonic amplitude (percent)

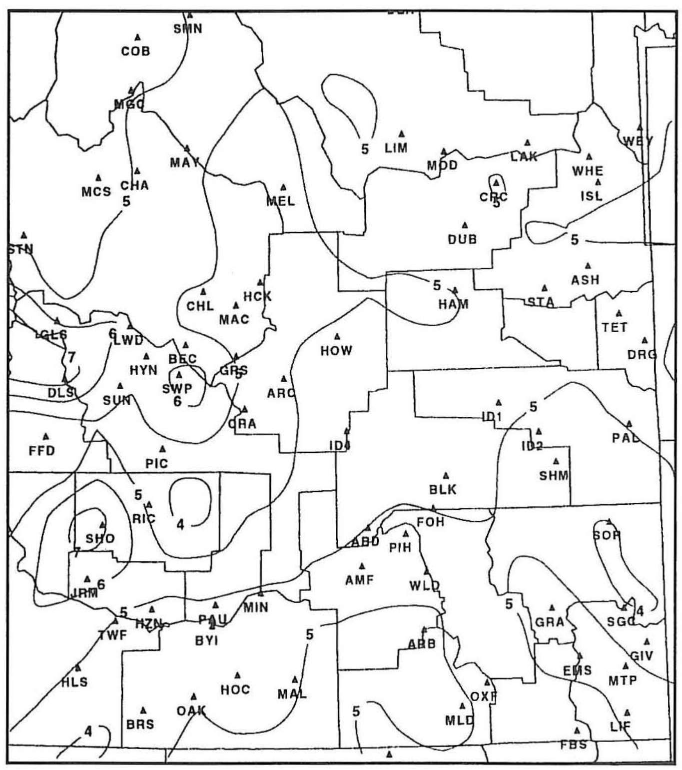

Fig. 19. Third harmonic phase (months)

40% contributions extends from Tetonia Experimental Station (TET) to Driggs (DRG); a local maximum of 40% is located near Palisades (PAL). Figure 19 indicates a general pattern of third harmonic maxima in January (t=1), May (t=5), and September (t=9) across most of eastern Idaho. (In the Magic Valley, third harmonic maxima occur from April (t=4) to July (t=7) but percentage contributions are less than 10%.) The area located from the Teton Range into the Caribou Highlands is less influenced by warm/cold season maxima related to Pacific cyclonic controls and Polar Jet transitions and to a much greater degree is influenced by large-scale orographic precipitation induced by westerly upslope of moist air along the east to southeast facing slopes of the Caribou Highlands. Thus, Fig. 18 indicates a west to east gradient from Idaho Falls 2 ESE (10%) to Palisades (40%) in the third harmonic amplitude data, suggesting another gradation in climate regimes, with a tendency for higher frequency seasonal precipitation events from the eastern part of the USRP to near the Teton Range (along the Idaho-Wyoming border) and extending into the Caribou Highlands. The time series for Palisades (Fig. 20) illustrates the strong tendency for three maxima and minima in the annual precipitation time series. The second (H2)

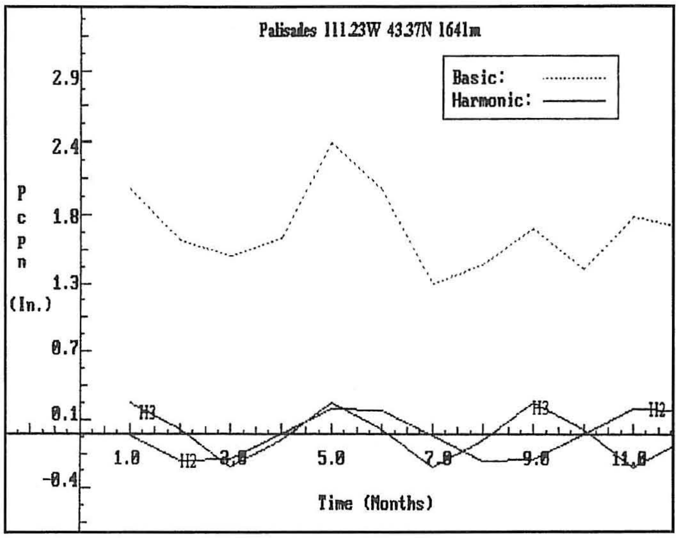

Fig. 20. Precipitation (in.) and harmonic time series for Palisades

and third (H3) harmonic curves reinforce each other during March (minimum) and May (maximum).

e. The higher harmonic amplitude percentage and phase charts

The fourth harmonic amplitude map (Fig. 21) indicates an area of 20 to 30% contributions from the fourth harmonic situated south of the Central Mountains with an absolute maximum of 32% near Arco 3 SW. The locally higher magnitudes near Howe and Arco 3 SW appear to be associated with their geographical locations at the terminations of the Big and Little Lost River Valleys, respectively (Fig. 1). The fourth harmonic phase chart (Fig. 22) displays the tendency for four maxima and four minima in the annual march of precipitation; it shows February (t=2), May (t=5), August (t=8), and November (t=11) maxima in these areas. Both Howe and Arco 3 SW may be influenced by both small-scale upslope and convergence due to the slight elevation in topography relative to the surrounding terrain and flow interaction between the SRP and central valleys. Bjorem (1969) noted that these varying wind flow patterns aid in the formation of squall line thunderstorms near Arco 3 SW during the spring and summer months.

The percentage contributions from fifth harmonic amplitudes are relatively small in eastern Idaho (not shown) and approach about 10% near Oakley (OAK); phase maxima occur in May. Contributions from the sixth harmonic amplitude and phase charts (not shown) are less than 5% across east Idaho indicating that salient bimonthly changes in the annual precipitation march, even over complex terrain, are very small.

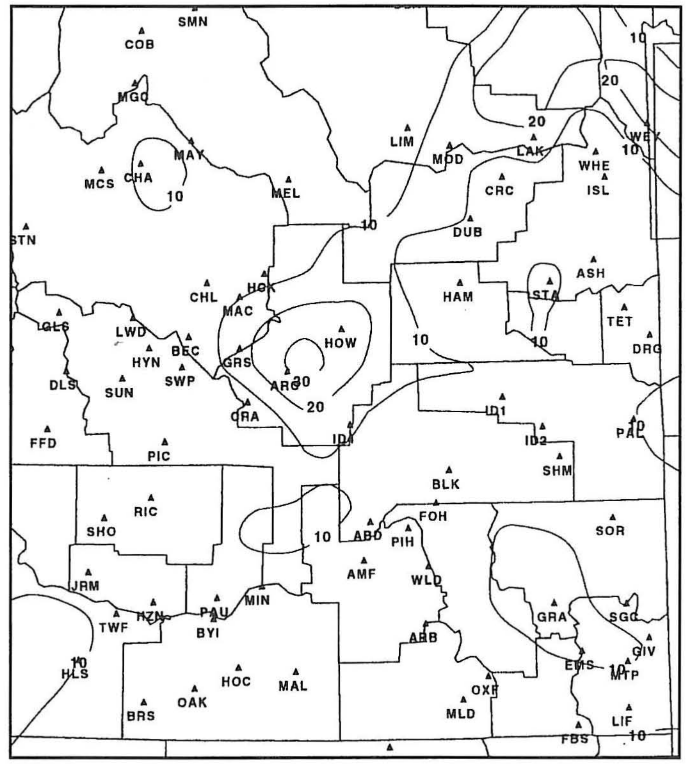

Fig. 21. Fourth harmonic amplitude (percent)

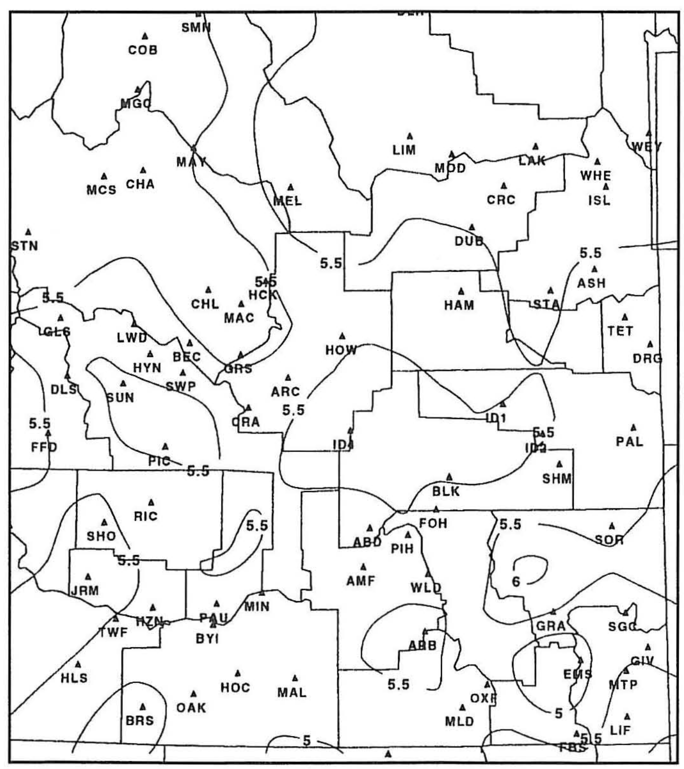

Fig. 22. Fourth harmonic phase (months)

5. Conclusions

The method of harmonic analysis was used to illustrate the intensity and phase of precipitation regimes in eastern Idaho using NCDC 30-year normals for 67 climate stations and 33 NRCS SNOTEL stations in eastern Idaho, including the conterminous regions of Montana, Utah, and Wyoming. Cold season precipitation maxima, as expressed by the first harmonic amplitudes, are evident in the Magic Valley, west Central Mountains, and Upper Snake Highlands. These maxima are highly correlated with Pacific cyclogenesis while summer minima are associated with the subsident influences of the Great Basin High (Trewartha 1981). The eastern part of the

Central Mountains exhibits strong summer maxima where terrain blocking inhibits winter precipitation, and warm season convection is more dominant versus cold season Pacific cyclonic controls. Phase transition regions in the first harmonic are evident from a January maximum at Stanley to a July maximum at May to a January maximum at Meadow Lake.

The meridionally oriented first harmonic summer maxima which intrudes from east of Howe to near Lima may reflect the northward extent of the summer monsoon, which originates over Arizona and New Mexico during June and July (Trewartha 1981). Moreover, salient first harmonics over the Lower Snake River Plain transition to well-defined second harmonics over the Upper Snake Plain, with an absolute second harmonic maximum near St. Anthony 1 WNW. The spring and fall maxima are influenced by the seasonal transitions of the North Pacific Polar Jet (Trewartha 1981). An area of strong third harmonics, situated from the eastern part of the Upper Snake River Plain to near the Idaho-Wyoming border and into the Caribou Highlands, appears to be associated with large-scale orographic precipitation forcing. This may be linked to westerly upslope of moist air along the windward sides of the Teton Range in western Wyoming. Finally, strong fourth harmonic amplitudes are observed near Howe and Arco 3 SW, possibly due to local upslope and convergence forced by terrain elevation differences and interaction of wind flow in the SRP with the Central Mountain Valleys. However, additional research is still needed to ascertain the precipitation mechanisms which produce the salient third and fourth harmonics in regions of varied terrain.

Acknowledgments

The author would like to thank NCDC and NRCS for providing the mean monthly precipitation normals. A special thanks to Jay Albrecht, Dr. Greg Johnson, Mark Mollner, Dean Hazen, and Rusty Billingsley for providing constructive comments on this paper.

Author

Thomas Andretta serves as lead forecaster at the NOAA/National Weather Service (NWS) Office at Pocatello/Idaho Falls, Idaho. He joined the NWS in May 1993 as a meteorologist intern at the NWS Office in Lake Charles, Louisiana and was promoted to journeyman forecaster at the NWS Office in Pocatello/Idaho Falls in April 1995. He graduated from the State University of New York at Stony Brook in 1988 with a B.S. in Atmospheric Science and in 1991 with a M.S. in Atmospheric Science. He wrote his Master's Thesis on precipitation perturbations in two versions of the Oregon State University Global Circulation Climate Model which featured variable ambient CO_2 concentrations. His area of expertise is in mesoscale meteorology and precipitation climatology. He has authored a recent manuscript in the June 1998 issue of Weather and Forecasting analyzing a boundary layer convergence zone event in the Snake River Plain of eastern Idaho.

References

Andretta, T.A., 1990: *An Analysis of Precipitation Perturbations in the 2 x CO_2 Climate Using a Global Circulation Model*, (M.S. thesis) 446 pp.

________, and D.S. Hazen, 1998: Doppler radar analysis of a Snake River Plain convergence event. *Wea. Forecasting*., 13, 482-491.

Astling, E.G., 1984: On the relationship between diurnal mesoscale circulations and precipitation in a mountain valley. *J. Appl. Meteor.*, 23, 1635-1644.

Bjorem, D., 1969: Eastern Idaho squall line. *Western Region Technical Attachment*, 69-29.

Fitzpatrick, E.A., 1964: Seasonal distribution of rainfall in Australia analyzed by Fourier methods. *Archiv. Meteor. Geophys. Bioklim.*, B., 13, 270-286.

Hastenrath, S.L., 1968: Fourier analysis of Central American rainfall. *Archiv. Meteor. Geophys. Bioklim.*, B., 16, 81-94.

Horn, L.H. and R.A. Bryson, 1960: Harmonic analysis of the annual march of precipitation over the United States. *Ann. Assoc Amer. Geogr.*, 50, 157-171.

Kendrew, W.G., 1922: *The Climates of the Continents*. Oxford University Press, New York, 473 pp.

Kirkyla, K.I. and S. Hameed, 1989: Harmonic analysis of the seasonal cycle in precipitation over the United States: A comparison between observations and a general circulation model. *J. Climate*, 2, 1463-1475.

Panofsky, H.A. and G.W. Brier, 1958: *Some Applications of Statistics to Meteorology*. The Pennsylvania State University, 128-134.

Potter, G.L. and W.L. Gates, 1984: A preliminary intercomparison of the seasonal response of two atmospheric climate models. *Mon. Wea. Rev.*, 112, 909-917.

Scott, C.M. and M.D. Shulman, 1979: An areal and temporal analysis of precipitation in the northeastern United States. *J. Appl. Meteor.*, 18, 627-633.

Trewartha, G.T., 1981: *The Earth's Problem Climates*, The University of Wisconsin Press, Madison, 371 pp.

Wilks, D.S., 1995: *Statistical Methods in the Atmospheric Sciences: An Introduction (International Geophysics, Vol. 59)*, Academic Press, 467 pp.

Winkler, J.A., B.R. Skeeter, and P.D. Yamamoto, 1988: Seasonal variations in the diurnal characteristics of heavy hourly precipitation across the United States. *Mon. Wea. Rev.*, 116, 1641-1658.